Evaluation of Sensitivity Improvements on a Tandem Mass Analyzer

Satendra Prasad,[1] Eloy R. Wouters,[1] Jean-Jacques Dunyach,[1] and Alexander A. Makarov[2]
[1]Thermo Fisher Scientific, San Jose, CA; [2]Thermo Fisher Scientific (Bremen) GmbH, Bremen, Germany

Thermo SCIENTIFIC

Overview

Purpose: Increasing the ion flux into a tandem mass analyzer to enhance sensitivity for quantitative analysis at high and nano-flow rates.

Methods: Gas throughput (Q) was more than quadrupled, downstream ion optics were modified, and gas pumping capacity was increased to accommodate the high Q and increased ion flux.

Results: Quantitative assays at high and nano-flow rates show increase in analyte signal, lower relative standard deviation (RSD), and superior limits of quantitation (LOQ) in comparison to the previous generation tandem mass analyzer.

Introduction

Using a large bore ion transfer tube or capillary combined with an electrodynamic ion funnel or stacked ring radio frequency (RF) ion guide has been a common practice to enhance the sensitivity of tandem mass analyzers. However, enlarging the capillary bore causes two complications that offset the sensitivity gain. First, it reduces the radial heat transfer to the flow channel which compromises the desolvation property of the capillary. An excessive amount of solvent clusters enter the mass analyzer and convolve low abundance analyte signal. Second, increasing the bore size yields highly collimated flow streamlines from the capillary that penetrate across the multiple differential pumping stages and into the mass analyzer. With the pumping capacity unmodified, the increase in gas load adversely affects the ability of RF fields to confine ions and the overall efficiency of ion transport decreases. In this study, however, we demonstrate an approach to more than quadruple the Q and gain sensitivity by using a novel high-capacity ion transfer tube (HCTT) and an electrodynamic ion funnel (IF) which when combined, either eliminate or reduce the two complications that arise from increasing Q on a tandem mass analyzer.

Methods

Samples containing several target compounds (Table 1) in crashed plasma were resolved using a Thermo Scientific™ Hypersil™ GOLD AQ 100 x 2.1 mm, 1.9 µm C18 column over an eight minute gradient that spanned from 95% aqueous (0.1% Formic Acid) to 95% acetonitrile (0.1% Formic Acid). Sample delivery and regulation of solvent composition was accomplished using a Thermo Scientific™ Ultimate™ 3000 LC pump and autosampler. Eluents were delivered at 500 µL/min into a Heated Electrospray Ionization (HESI) ion source.

A separate assay, including constituents of Bovine Serum Albumin (BSA) and Enolase (Table 2) diluted in *E. coli* digest was used to characterize sensitivity at a nano-flow rate (300 nL/min). Five target constituents were resolved using a Thermo Scientific™ EASY-Spray 75 µm x 15 cm, C18, 3 µm, 100 Å column over a 30 minute gradient controlled by a Thermo Scientific™ EASY-nLC II pump. Composition of the mobile phase was varied in multiple steps from 5% aqueous (0.1 Formic Acid) to 95% methanol (0.1% Formic Acid).

The assays were analyzed on the Thermo Scientific™ TSQ Quantiva ™ mass spectrometer equipped with a Thermo Scientific™ Easy-Max NG high flow or a Thermo Scientific™ Nanospray Flex NG ion source, ion funnel, ion beam guide with a neutral blocker, and the Thermo Scientific™ HyperQuad™ quadrupole mass filter. The HCTT could be interchanged with a standard ion transfer tube for comparative purposes.

FIGURE 1. A schematic showing key differences in upstream ion optics between the new high sensitivity and previous generation triple quadruple.

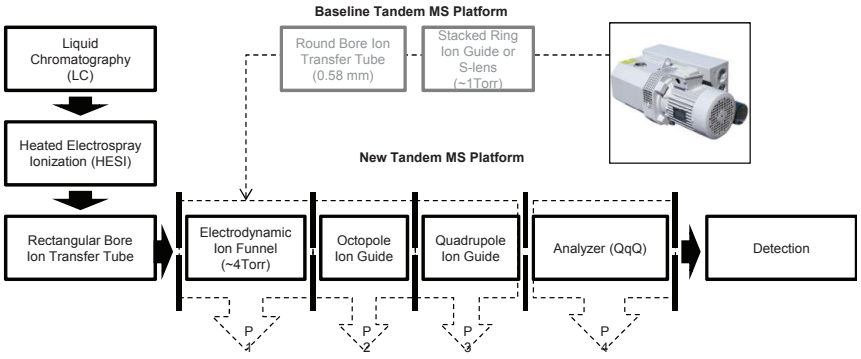

Results

Novel Features of the High Capacity Ion Transfer Tube (HCTT)

Gas Dynamics

When the system is equipped with a round bore ion transfer tube (d=0.58mm) that has a conductance of ~ 1.4 L/min and a rough pumping capacity of 55 m^3/hr, the local pressure in each of the pumping chambers are as follow (Figure 1): P1 = ~1.5 Torr, P2 = ~120 mTorr, P3 = ~1.5 mTorr, and P4 = ~4.0 x 10^{-6} Torr. However more than quadrupling Q with a HCTT and doubling the pumping capacity only elevated the pressure in the IF to ~ 4Torr with little change in pressure in the downstream chambers (P2-P4). This was difficult to accomplish at comparable Q with a round bore capillary. The correlation between the HCTT and the reduction in gas load is treated as a novel property and was studied in detail with computational fluid dynamics (CFD).

Figure 2 shows the orientation of the HCTT when fitted into the mass spectrometer (MS) and was found to be optimum for sampling of ions from the HESI ion source (not shown). Computational fluid dynamics (CFD) calculations were accomplished for the above orientation of the HCTT.

FIGURE 2. Showing assembly of HCTT and an IF (left) and the orientation of width (W) and height (H) dimension on a YX plane (right).

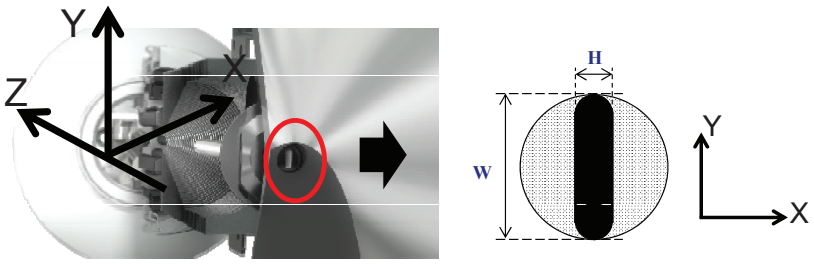

Figure 3 shows the propagation of the Mach disc across the YX plane (side view) and the ZX plane (top view) from the HCTT into an IF that were contained in the first pumping stage (P1). The overall behavior of the gas expansion in the YX plane was anticipated, however, the ZX plane shows a radial expansion of the Mach disc which is not seen in the YX plane. A reconstruction of the CFD data in a three dimension space (not shown) reveals that the Mach disc was asymmetrical in shape. The asymmetry causes a radial dispersion of the gas streamlines away from center axis towards the edges of the RF electrodes, and reduces the flux of gas molecules going into the downstream pumping stages.

FIGURE 3. Two dimensional contour plots showing the gas flow profile developing from a HCTT and into an IF in the YX (left frame) and ZX plane (right frame).

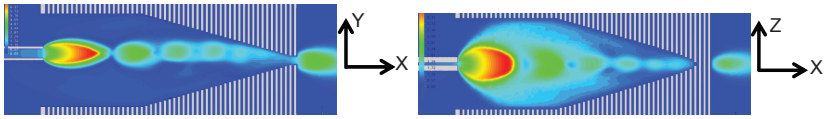

In Figure 4, the graph on the left shows a linear relationship between cross sectional area and pressure for both the standard capillary and the HCTT in P1. A similar trend is seen in P3 but not for the HCTT types. For the latter capillaries, the pressure in P3 is resilient to throughput increase. This is consistent with the CFD results that implied reduction in axial flux of gas molecules owing to the radially polarized Mach disc.

FIGURE 4. Pressure measured in P1 and P3 as a function of cross sectional area for a range of round bore ion transfer tubes (red diamonds) and a range of rectangular bore ion transfer tubes (blue triangles).

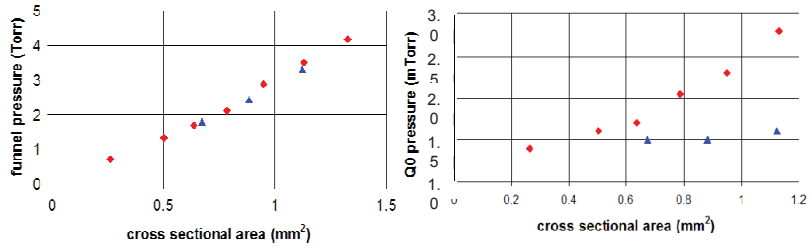

Throughput increase and desolvation

Another advantage of having a HCTT is to not sacrifice the ability to desolvate ions, particularly those arising from a high aqueous LC stream. Maintaining the height dimension comparable to 0.6 mm, which is accepted as a standard for optimum desolvation on the current generation mass spectrometers, can ensure a good radial heat transfer. This was thoroughly evaluated by measuring the response of nine constituents (Table 1) across multiple flow rates (0.3 mL/min to 2.0 mL/min) with a standard and HCTT.

FIGURE 5. A Total Ion Chromatogram (TIC) of nine constituents analyzed at high flow rate with a HESI-LC-SRM system.

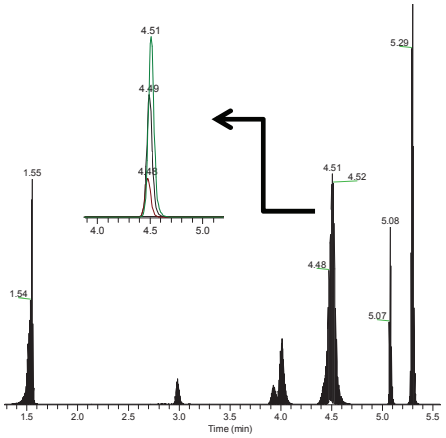

Table 1. List of nine compounds and product ions monitored during SRM analysis.

Name	$[M+H]^+$	Product Ions (CE)	RT (min)
Oxycodone	316.15	241.08 (27)	1.54
Buprenophine	468.31	414.2 (36) 396.3 (36)	2.98
Paroxetine	330.15	192.12 (19)	4.01
Clonazepam	316.05	270.06 (24)	4.48
Verapamil	455.29	165.1 (25)	4.51
Ketoconazole	531.16	489.1 (29)	3.93
Alprazolam	309.09	281.1 (25)	4.49
Reserpine	609.28	195.1 (38) 174.1 (41)	5.08
Clopidogrel	322.07	212 (14)	5.30

The TIC in Figure 5 shows the separation of compounds over an eight minute multi-step gradient. Oxycodone (mass-to-charge ratio or *m/z* = 316.15) eluted during a LC solvent composition of ~70% aqueous and 30% acetonitrile. Any difference in desolvation property between the capillaries will be reflected in the peak area as a function of LC flow rate. But the results (Figure 6) show near identical trend between the capillaries confirming no compromise in desolvation of the ions when using the HCTT. Similar trends were observed for all the analytes in the TIC.

FIGURE 6. A description of the LC gradient profile employed to resolve the nine compounds contained in crashed plasma (top frame). Bar graphs show a change in the Oxycodone peak area with increasing LC flow rate for LC-SRM analysis using a standard round bore capillary (0.58 mm) and HCTT (0.6 mm x 2.0 mm).

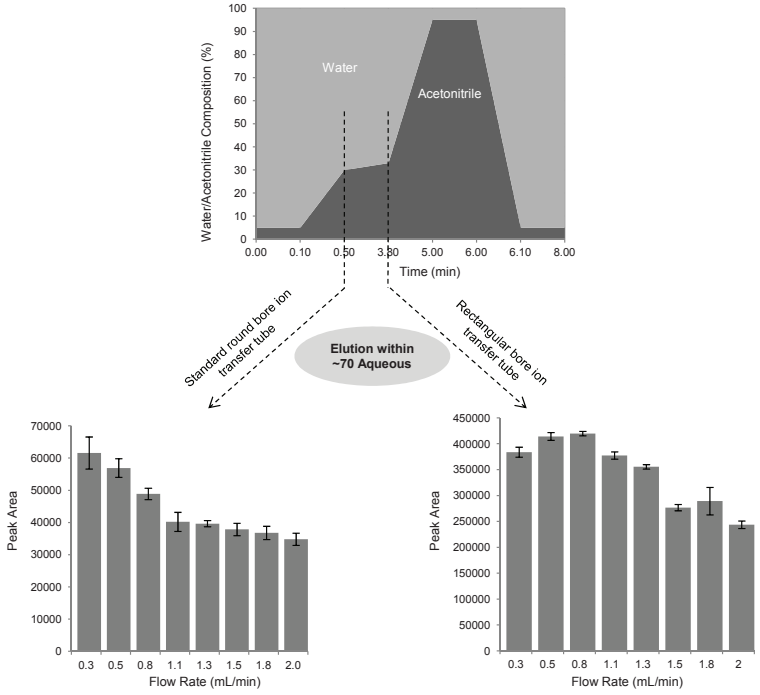

Sensitivity increment and gain in LOQ's in HESI-LC-SRM mode

High Flow Rate:

Figure 7 shows peak area (not normalized to ISTD) versus femtograms of compounds deposited on the LC column for Alprazolam and Verapamil. The increase in signal flux (*S*) for the two compounds varied between 8.6X to 14X which exceeds the throughput of the HCTT and is explained by a favorable alignment between the HESI spray and HCTT which facilitates sampling of a greater fraction of the ion spray that is usually inaccessible when using a round bore capillary.

At low levels, improvement in the LOQ was observed using HCTT (red trace) over the standard capillary (black trace). The gain in LOQ scaled as √S which was anticipated owing to increase in chemical noise. This was also consistent when %RSD's were compared at fixed levels. For instance, in case of Alprazolam *S* ~14X, the expected gain in LOQ was √S= 3.9X but comparison of the RSD at 100 fg revealed ~2X improvement which was consistent with a 2X improvement in LOQ.

FIGURE 7. Plots of peak area (not normalized to ISTD) versus femtograms of Alprazolam (309→ 281.15) and Verapamil (455.3→ 165.1) injected on LC column for analysis with HCTT (red) and standard capillary (black). Inserts (right) shows selected ion chromatogram at levels that are the LOQ when using standard capillary: HCTT (red trace) and standard capillary (black trace).

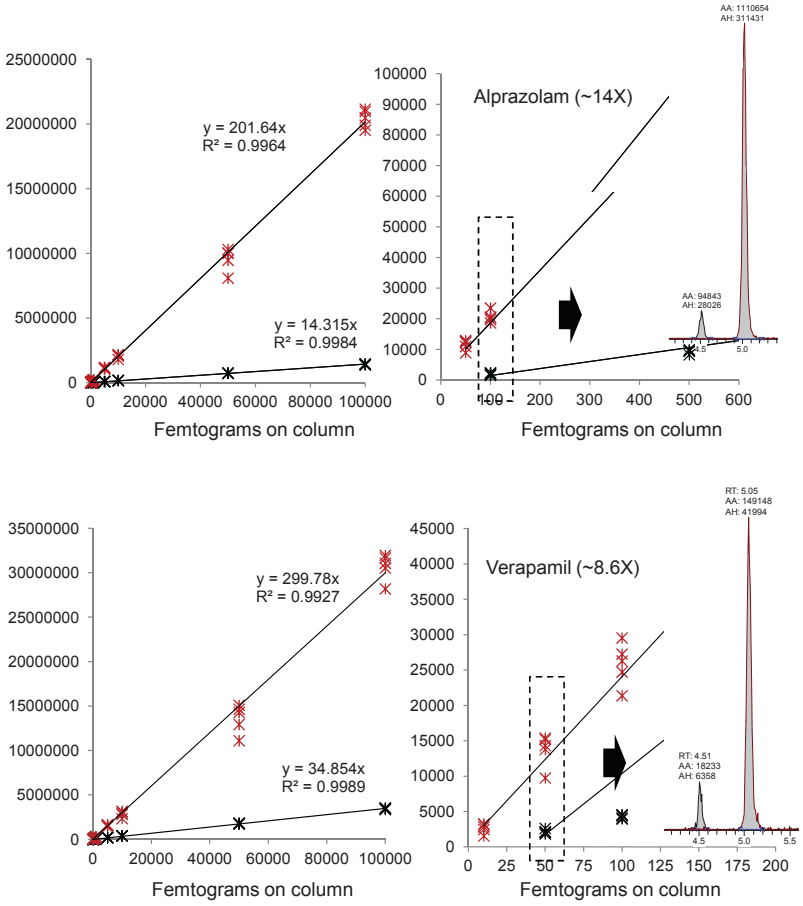

Similar correlation between *S*, RSD, and LOQ was observed for Paroxetine, Reserpine, and Clopidogrel (Table 2). Between the standard capillary and the HCTT, Paroxetine showed no improvement in LOQ but ~2X improvement in %RSD was observed. Although the compounds Oxycodone, Buprenorphine, Clonazepam, and Ketoconazole were expected to improve in LOQ by 2.6X-3.4X, the chromatograms and statistical treatment of the data showed a 10X improvement in LOQ. The discrepancy between the expected and experimental gain can be explained by large increment in concentration levels at the low levels in the calibration curve. Steps in the sample dilution at the low levels should be matched with the expected gain:2-3X.

Table 2. List of increase in signal flux, the estimated and experimental gain in LOQ for the nine compounds.

Compound	Difference in ion flux (S)	Δ %RSD at comparable level (fg)	Expected LOQ improvement (√S)	LOQ improvement
Paroxetine	6.5X	1.8X	2.5X	none
Verapamil	9.0X	4.2X	3.0X	5X
Alprazolam	14.0X	2.0X	3.7X	2X
Clopidogrel	5.0X	~1.0X	2.2X	5X
Reserpine	11.5X	2.6X	3.4X	5X
Buprenorphine	7.0X	2.0X	2.6X	10X
Clonazepam	8.5X	3.0X	3.0X	10X
Ketoconazole	10.0X	2.7X	3.2X	10X
Oxycodone	9.0X	2.0X	3.0X	10X

Nano-flow rate:

Figure 8 shows the separation of the six constituents from BSA and Enolase mixture which were compared for increase in signal flux between a standard and HCTT. A 2X to 3.5X enhancement in peak area was observed (bar graphs) across the six constituents which correlated with the increase in Q.

FIGURE 8. A Total Ion Chromatogram (TIC) showing the elution of six constituents from a mix of BSA and Enolase at a flow rate of 300 nL/min.

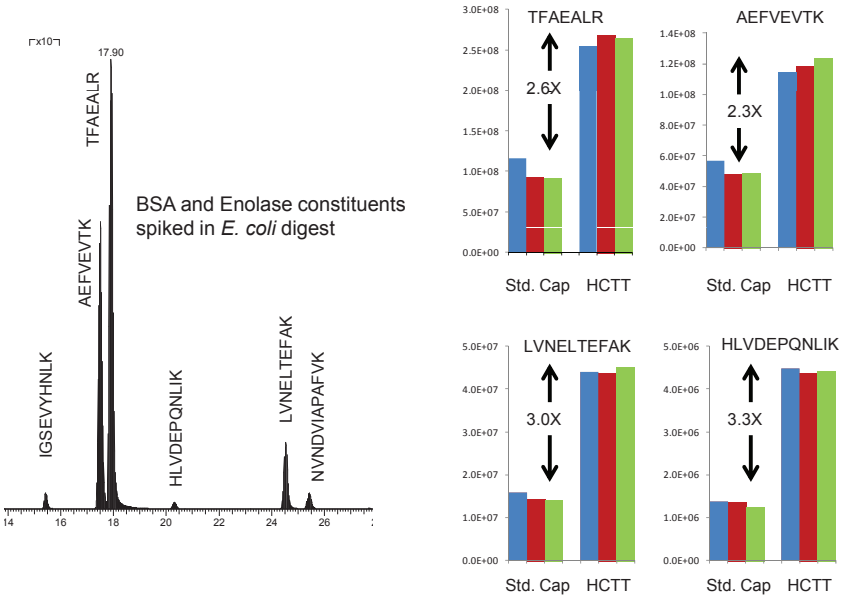

Conclusion

- Throughput was more than quadrupled using a rectangular bore in the ion transfer tube and an ion funnel.
- The rectangular flow channel yielded excellent desolvation of ions.
- Sampling of ions from the HESI source was superior with the HCTT.
- The ion funnel efficiently captured spatially dispersed ions from the HCTT.
- Signal flux increased both in nano and high flow rate conditions which translated into improvement in ion statistics, RSD, and LOQ.

Acknowledgements

The authors would like to acknowledge Reiko Kiyonami for assistance with sample preparation and Marcus Miller for technical assistance with LC.

www.thermofisher.com

Africa-Other +27 11 570 1840
Australia +61 3 9757 4300
Austria +43 1 333 50 34 0
Belgium +32 53 73 42 41
Canada +1 800 530 8447
China +86 10 8419 3588
Denmark +45 70 23 62 60
Europe-Other +43 1 333 50 34 0
Finland/Norway/Sweden +46 8 556 468 00
France +33 1 60 92 48 00
Germany +49 6103 408 1014
India +91 22 6742 9434
Italy +39 02 950 591
Japan +81 45 453 9100
Latin America +1 561 688 8700
Middle East +43 1 333 50 34 0
Netherlands +31 76 579 55 55
New Zealand +64 9 980 6700
Russia/CIS +43 1 333 50 34 0
South Africa +27 11 570 1840
Spain +34 914 845 965
Switzerland +41 61 716 77 00
UK +44 1442 233555
USA +1 800 532 4752

Thermo SCIENTIFIC

Part of Thermo Fisher Scientific

ASMS13_Th084_SPrasad_E 07/16S